J. Membrane Biol. 71, 149–161 (1983)

The Journal of
Membrane Biology

The Mechanism of Anion Transport Across Human Red Blood Cell Membranes as Revealed with a Fluorescent Substrate: II. Kinetic Properties of NBD-Taurine Transfer in Asymmetric Conditions

O. Eidelman and Z.I. Cabantchik

Department of Biological Chemistry, The Hebrew University of Jerusalem, Institute of Life Sciences, 91904 Jerusalem, Israel

Summary. The transport of inorganic anions across human red blood cell membranes is accomplished by a carrier-like mechanism which involves an electroneutral and obligatory one-for-one anion exchange. The transport kinetics were described by models that involve alternation of single transport sites between the two membrane surfaces. These models predict that each carrier shows either an inward-facing E_i or an outward-facing E_o, conformation, each capable of binding either a monovalent anion or a divalent anion+a proton, to yield an electroneutral translocating complex. Unidirectional transport rates provide, therefore, a measure for the relative concentration of carriers at a given membrane surface. In the present work we assessed how modulation of the transmembrane distribution of carriers by the anion composition of cells and media, and by pH, affect the anion transport system. We have set the system in asymmetric conditions with respect to anions, so that a fast transportable anion (e.g., chloride) was present in one side of the membrane and slow transportable anions (e.g., sulfate, phosphate, oxalate, isethionate, gluconate, HEPES) were present on the other side of the membrane. The skewed distribution of carriers induced in these conditions were assessed by two methods: 1) NBD-taurine transfer which provided a measure for $[E_i]$, the monovalent inward-facing form of the carrier, and 2) inhibition of NBD-taurine transfer by the specific impermeant and competitive inhibitor 4,4′-dinitro-2,2′-stilbene disulfonic acid (DNDS), which provided a measure for the availability of the carrier at the outer membrane surface. In the various symmetric and asymmetric conditions, we found marked differences in transport rates and transport profiles as well as in the susceptibility of the system to inhibition by DNDS. Direct binding studies of DNDS to cells in the various asymmetric conditions supported the conclusion derived from transport studies that transport sites can be recruited towards the membrane surface facing the slow transportable anions.

Key Words anion exchange · fluorescent studies · membrane permeability · red blood cells · conformational states

Introduction

In the previous work [9] we demonstrated that the fluorescent probe NBD-taurine, in conjunction with the CMTF[1] method, provides a valuable tool for measuring anion transfer across human erythrocyte membranes and for probing its molecular mechanism. The kinetic information obtained by the above technique was interpretable in terms of the anion carrier model [4, 11, 15], which displays obligatory, electrically silent exchange properties [15] and a ping-pong type of kinetics [12]. The model postulates that each carrier molecule contains a single transport site which alternates between two conformational states, one outward facing and one inward facing [14, 18]. Each of these states is populated by the unloaded and loaded (i.e., anion-complexed) forms of the carrier. Since anion translocation is an electrically silent phenomenon, it is assumed that the major route of carrier translocation is via the complexed electroneutral form [11]. An interesting mechanistic feature of the above model, which was first indicated by Dalmark [6] and recently reviewed by Knauf [15, 16] is that the transmembrane distribution of unloaded carrier forms depends largely on the relative concentrations of anions at the two membrane surfaces. At equilibrium this corresponds to the Donnan ratio.

In the present work we attempted to gain some insight into how the above distribution is modulated by the relative concentrations of

[1] *Abbreviations used:* CMTF, continuous monitoring of transport by fluorescence; DNDS, 4,4′-dinitro-2,2′-stilbene-disulfonic acid; HEPES, N-2-hydroxyethylpiperazine-N′-ethano-sulfonic acid; l.t., latent time; a.l.t., after latent time; MES, 2[N-morpholino]ethane sulfonic acid; NBD-taurine, N(*n*-aminoethylsulfonate)-7-nitrobenz-2-oxa-1,3-diazole; PBS, phosphate-buffered saline (NaCl 147 mM, phosphate 20 mM, pH 7.4); TCA, tri-chloro-acetic acid; TPB, tetraphenyl boron; TPP, tetraphenyl phosphonium; Tris, tris(hydroxymethyl)amino methane.

0022-2631/83/0071-0149 $02.60

anions present in the system. The transmembrane distribution was probed by the CMTF method which gives a measure of the inward-facing form of the unloaded carrier, and by inhibition and binding studies using the impermeant and anion-specific probe DNDS [1, 2] which interacts only with the outward-facing form of the carrier. Both approaches provided information which supports the idea of transmembrane conformational states of the anion carrier as predicted from the ping-pong mechanism [5, 12].

Materials and Methods

The sources of chemicals and radiochemicals used in this work are essentially the same as those described in the previous work [9].

Preparation of Cl-Loaded Cells

Red cells from freshly withdrawn blood or recently outdated blood (obtained from Shaarei Zedek Medical Center) were washed with PBS (148 mM NaCl, 20 mM phosphate, pH 7.4) until free of contaminating buffy coat. The cells were subsequently washed and resuspended in the medium of choice, as indicated.

Preparation of SO_4-Loaded Cells and of SO_4: Cl-Loaded Cells

SO_4-loaded cells were prepared by incubating washed cells (3% hematocrit) in SO_4 medium (usually 100 mM, Na_2SO_4, and either 20 mM Na-phosphate or 20 mM MES, pH 7.4, or as otherwise indicated) for 30 min at 37 °C. The cells were spun down, resuspended in the same medium and incubated for an additional 30-min period at 37 °C. SO_4:Cl-loaded cells were prepared by a similar procedure, except that the incubation media included different concentrations of NaCl replacing isoosmotically the Na_2SO_4, and the final pH was 6.9. After the above incubation periods, the cells were incubated for several hours at 20 °C to allow further equilibration of anions. The choice of pH 6.9 (20 °C) was in order to set the system at Donnan equilibrium with respect to anions at a Donnan ratio of 1 [7]. Change of intracellular pH, determination of cell volume and determination of Donnan ratio were performed essentially as described in the preceding work [9].

Flux Measurements

The efflux of NBD-taurine from either Cl-, SO_4- or SO_4:Cl-loaded cells was followed by the CMTF method as previously described [8, 9]. Briefly, cells loaded with inorganic anions, as described above, were subsequently incubated with 1 mM NBD-taurine dissolved in the same medium, at 37 °C for at least one hour (final hematocrit 10%). In most cases this incubation period was sufficient for transcellular equilibration of the fluorescent probe. At the end of this period the NBD-taurine-loaded cells were brought to the final temperature of the efflux experiment and they were incubated for an additional 30-min period. Prior to flux measurements a 50-µl aliquot of cells was washed twice with 1 ml-portions of ice-cold, unbuffered isotonic Na_2SO_4 in order to remove extracellular NBD-taurine. Fluxes were initiated by injection of 50-µl cell suspensions (approximately 1% hematocrit) into 2 ml of flux medium, which were placed in the cuvette of the spectrofluorimeter. The medium was flushed with N_2 for a half hour prior to fluxes and during fluxes in order to remove CO_2. The fluorescence intensity was recorded with time. To terminate the flux, an aliquot of the detergent NP-40 was added (0.025% wt/vol, final concentration) in order to lyse the cells and release the remaining intracellular probe. The fluorescence intensity at the time of addition of cells and after addition of detergent are denoted $F(o)$ and $F(\infty)$, respectively. The $F(\infty)-F(o)$ gives a measure of the amount of NBD-taurine present in the cells at zero time ($t=0$).

Fluxes of NBD-taurine were monitored either in a Perkin-Elmer MPF-4 spectrofluorimeter or in a Spex Fluorolog II. With the latter, the fluorescence was measured in the photon counting mode and the raw data was stored in a microprocessor as counts accumulated over successive 5-sec intervals ($F(t)$). The raw data were used to derive the instantaneous rate parameter $k_{inst}(t)$ at each $F(t)$ point along the time profile [9]:

$$k_{inst}(t) = -\frac{d}{dt}\ln\{[F(\infty)-F(t)]/[F(\infty)-F(o)]\}. \quad (1)$$

With the Perkin-Elmer instrument the kinetic data were calculated as initial efflux rates v (pmol/min/cell) from the slopes of the recorder tracings of $F(t)$ versus time t [9]:

$$v = \frac{f}{N}\frac{dF}{dt}(t\to 0) \quad (2)$$

where $\frac{dF}{dt}(t\to 0)$ is the initial slope of the fluorescence trace, f is the calibrated factor for conversion of fluorescence intensity into NBD-taurine concentration and N is the number of cells present in the cuvette (calculated from the 410 nm absorbance, *see* ref. [9]). For the case of NBD-taurine fluxes in symmetric conditions and/or in conditions giving exponential profiles, the rate constants $k(\text{min}^{-1})$ of NBD-taurine efflux were determined as

$$k = \frac{1}{F(\infty)-F(o)}\frac{dF}{dt}(t\to 0). \quad (3)$$

For the case of NBD-taurine efflux in asymmetric conditions, in which case the profiles were not of an exponential nature, we used the slope in the quasi-linear phase of the fluorescence trace for computing the rate constant (cf. Fig. 1). In order to compensate for the differences in the internal concentration S_i of NBD-taurine at Donnan equilibrium at various pH values, the v values were normalized to 1 mM NBD-taurine concentration ($\bar{v} = v/S_i = v/rS_o$, where $S_o = 1$ mM). This correction is valid, inasmuch as it has been shown that at 1 mM the apparent Michaelis constant of NBD-taurine $K_S > S_i$ [10].

Flux Measurements in the Presence of Inhibitors

Red blood cells were pre-equilibrated with Cl media (mM: 75 NaCl, 75 KCl, 10 Tris, 5 HEPES, 5 MES, pH as indicated) or with SO_4 media (50 mM Na_2SO_4, 50 mM K_2SO_4 replacing the above Cl salts), and were sub-

sequently loaded with NBD-taurine (1 mM final concentration) as indicated in previous sections. Efflux was measured by the CMTF method, in either the Cl or SO_4 media, containing various DNDS concentrations, and the same pH as the pre-equilibration medium (30 °C). For each experimental condition the rate constants k were used for constructing Dixon plots [21] of $1/k$ versus [DNDS]. For the case of Cl-loaded cells and SO_4 medium ($Cl_i - SO_{4_o}$), two apparent inhibition constants ($K_{i\text{-app}}$) were determined, one which measures the effect of DNDS on the latent time l.t. of NBD-taurine efflux, and the other which measures the effect of DNDS on the slope of the linear phase of the CMTF tracing, namely, after the latent time (a.l.t.). The first was determined from the plot of l.t. versus [DNDS]. Data were analyzed by linear regression analysis on a Wang PCSII calculator.

Measurements of DNDS Binding to Cells in Symmetric and Asymmetric Conditions

Red blood cells equilibrated with the indicated media were brought to a 40% hematocrit suspension and kept on ice. Aliquots of 1 ml cell suspension were added to 50 µl of media, containing various concentrations of DNDS, and placed in a 1.5 ml microfuge tube. The suspensions were thoroughly vortexed and spun down in an Eppendorf microcentrifuge ($12{,}000 \times g \times 20$ sec). The concentration of DNDS in the supernate was determined from the absorbance at 353 nm [2], after acid precipitation (TCA 5% final). The acid precipitation did not lead to either changes in DNDS absorbance or co-precipitation of DNDS with released hemoglobin [2].

The binding properties of DNDS to cells were calculated from:

$$T = n\frac{N[F]}{K_{B\text{-app}} + [F]} + V[F] \tag{4}$$

where T is the total amount of DNDS in the tube, $[F]$ is the concentration of free DNDS, n is the number of cells in each tube determined by the 410 nm absorbance of a 1:1000 water dilution of the above suspension [9], V is a parameter that accounts for the extracellular volume and the nonspecific (i.e., nonsaturable) component of binding, N is the number of binding sites and $K_{B\text{-app}}$ is the binding constant. The data were analyzed by a nonlinear regression program [9] according to the above equation, yielding the best fit parameters of N, $K_{B\text{-app}}$ and V.

Results and Discussion

NBD-Taurine Transfer under Asymmetric Conditions

The transfer of NBD-taurine from cells to medium was interpreted to be a function of the concentration of E_i, the unloaded monovalent form of the carrier in the inward-facing conformation [9]. A possible means to assess this idea is to set up experimental conditions whereby the transmembrane distribution of carriers, hence, the relative concentration of E_i, is modified. We have chosen to study NBD-taurine transfer from cells (i) to medium (o) in conditions leading to different carrier distributions: from Cl-loaded cells into Cl or SO_4 medium (i.e., $Cl_i - Cl_o$ and $Cl_i - SO_{4_o}$, respectively) and from SO_4-loaded cells into Cl or SO_4 medium (i.e., $SO_{4_i} - Cl_o$ and $SO_{4_i} - SO_{4_o}$, respectively). In the symmetric media, the E_i/E_o ratio (i.e., the transmembrane ratio of monovalent forms of the carrier) was shown to be a function of the anion and proton distribution [14, 15]. In these conditions equilibrium is established with respect to the predominant anion and to protons, so that the carrier distribution does not change with time; thus, NBD-taurine fluxes can be described by a single exponential function as expected for a simple tracer decay system. In the asymmetric $Cl_i - SO_{4_o}$ and $SO_{4_i} - Cl_o$ conditions, no such equilibrium exists and, since the carrier transports Cl at about four orders of magnitude faster rates than SO_4, the implications are that the initial distribution of transport sites should be skewed with the majority of these sites facing the SO_4 medium [14]. As anions exchange with each other, the skewness of the distribution should decrease progressively until reaching a steady value at Donnan equilibrium.

In a recent work Jennings [14] approached the question of carrier distribution by following SO_4 fluxes. In this work the test anion for E_i is NBD-taurine. The efflux profiles of NBD-taurine under asymmetric $Cl - SO_4$ conditions show two features which are distinctly different from those found in symmetric $Cl_i - Cl_o$ and $SO_{4_i} - SO_{4_o}$ conditions [9]: They do not fit to a single exponential function (Fig. 1, *B–C*) and they are markedly different in $Cl_i - SO_{4_o}$ as compared with $SO_{4_i} - Cl_o$ conditions.

The data are analyzed in terms of the instantaneous rate parameter $k_{\text{inst}}(t)$ (Fig. 1, *C*) which is defined as:

$$k_{\text{inst}}(t) = -\frac{d}{dt}\ln\left\{\frac{F(\infty) - F(t)}{F(\infty) - F(o)}\right\}$$

$$= \frac{1}{F(\infty) - F(t)}\frac{d}{dt}F(t).$$

(Eq. 1, *see* Materials and Methods.)

The value of $k_{\text{inst}}(t)$ is closely related to the normalized flux rate $\bar{v} = \frac{v}{S_i}$ [9], since $\frac{d}{dt}F(t)$ is proportional to the flux rate v and $F(\infty) - F(t)$ is proportional to the concentration of S_i at time t (cf. accompanying work [9], Eq. 8).

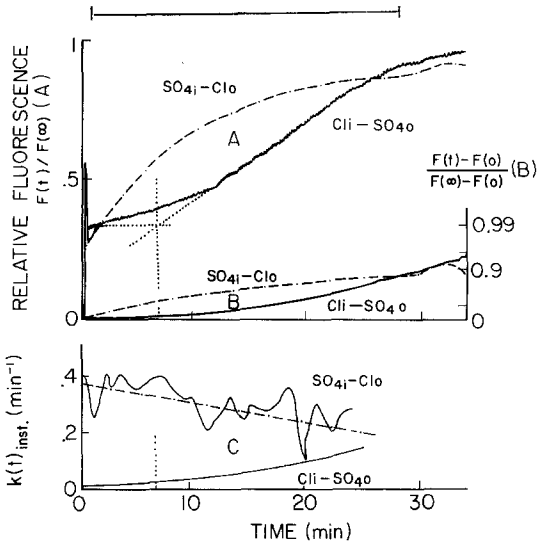

Fig. 1. NBD-taurine efflux (asymmetric $i-o$ conditions). Red blood cells were pre-equilibrated at 30 °C in Cl medium (Cl_i: 150 mM NaCl, 10 mM HEPES, pH 7.4), and subsequently loaded with 1 mM NBD-taurine and jetted into a cuvette containing CO_2-free sulfate medium (SO_{4_o}: 110 mM Na_2SO_4, 10 mM HEPES, pH 7.4) at 30 °C. The efflux of NBD-taurine was followed by the CMTF method on a SPEX Fluorolog II instrument. In a similar fashion we followed the efflux of NBD-taurine from SO_4-loaded cells (SO_{4_i}) also loaded with 1 mM probe into Cl medium (Cl_o) at 30 °C. *A*. Traces of NBD-taurine fluorescence as a function of time are given as $F(t)/F(\infty)$, where $F(t)$ and $F(\infty)$ are the fluorescence intensities at time t and at $t \to \infty$, respectively. The continuous line denotes the profile in $Cl_i - SO_{4_o}$ conditions, whereas the discontinuous line denotes the profile in $SO_{4_i} - Cl_o$ conditions. The dotted lines demonstrate the graphic method used for measuring the time required for the NBD-taurine flux to reach a steady value in $Cl_i - SO_{4_o}$ conditions (the latent time l.t.). This time was obtained by extrapolation of the $F(t)$ line to the $F(o)$ level (horizontal dotted line). *B*. The logarithmic plots of $[F(\infty)-F(t)]/[F(\infty)-F(o)]$, calculated from the above curves by the Datamate microprocessor, are shown as a function of time. *C*. Time dependence of the instantaneous rate parameters

$$k(t)_{\text{inst.}} = \frac{d}{dt} \ln \left\{ \frac{[F(\infty)-F(t)]}{[F(\infty)-F(o)]} \right\}$$

obtained from the two efflux curves shown in *A*. The discontinuous line represents the linear least-squares fit of $k(t)_{\text{inst.}}$ versus time for the $SO_{4_i} - Cl_o$ system

The values of k_{inst} at $t=0$ (pH 7.0, 30 °C) were markedly different for the two asymmetric systems, 0.008 min^{-1} for $Cl_i - SO_{4_o}$, as compared with 0.38 min^{-1} for $SO_{4_i} - Cl_o$ (Fig. 1 *C*). They also differed from k_{inst} obtained under symmetric conditions (pH 7.0, 30 °C), 0.07 min^{-1} for $Cl_i - Cl_o$ and 0.18 min^{-1} for $SO_{4_i} - SO_{4_o}$ [9]. While in symmetric conditions a single k_{inst} described the entire flux [9], in $SO_{4_i} - Cl_o$ conditions $k_{\text{inst}}(t)$ was found to decrease as efflux progressed, and in $Cl_i - SO_{4_o}$ conditions the profile was even more complex in that it showed an initial lag or latent phase of relatively slow transfer rate (or small k_{inst}) and a subsequent phase of gradual increase in k_{inst}. Each of these phases, found in $Cl_i - SO_{4_o}$ conditions, has a characteristic time, the first defined as the latent time of transfer (l.t.) and the second as after the latent time (a.l.t.). The graphic method used for the determination of l.t. is depicted in Fig. 1 (dotted lines). Latent phases were found (*not shown*) not only in $Cl_i - SO_{4_o}$ conditions but also whenever fast transportable anions were present intracellularly (e.g., F^-, Cl^-, Br^-) and slow transportable anions were present extracellularly (e.g., SO_4^{2-}, HPO_4^{2-}, oxalate, isethionate, gluconate, HEPES).

As stated above, in these conditions the system is expected to show a skewed distribution of carrier transport sites, with most of these sites facing outward and very few E_i available for NBD-taurine transfer. As SO_4 exchanges for intracellular Cl_i, the skewed distribution relaxes and the kinetic properties of NBD-taurine efflux gradually approach those found in $SO_{4_i} - SO_{4_o}$ conditions. In the reversed conditions (i.e., $SO_{4_i} - Cl_o$), the skewed distribution of carrier transport sites is induced in the opposite direction, so that most E sites are facing inward initially, leading to a fast exit of NBD-taurine. Again, as the skewed distribution relaxes, NBD-taurine transfer approaches the rate found in $Cl_i - Cl_o$ conditions. This result is essentially analogous to those obtained by tracer fluxes of $SO_4 - Cl$ heteroexchange, which are also interpretable in terms of skewed distribution of carriers [14]. Our results are also compatible with the idea that the fluorescent substrate is transported only by the form of the carrier mechanism that is responsible for monovalent anion exchange [9].

In order to assess further the role of carrier distribution in anion transport, we set out to study how the kinetic properties of NBD-taurine transfer reflect the modulation of the above distribution by various factors. In asymmetric $Cl - SO_4$ conditions, a means to modulate the distribution of carriers is by gradual supplementation of Cl to the SO_4-containing compartment, thus leading to dissipation of the skewed distribution in favor of a more even distribution of carriers. For $Cl_i - SO_{4_o}$ conditions, addition of Cl to the external medium induced a

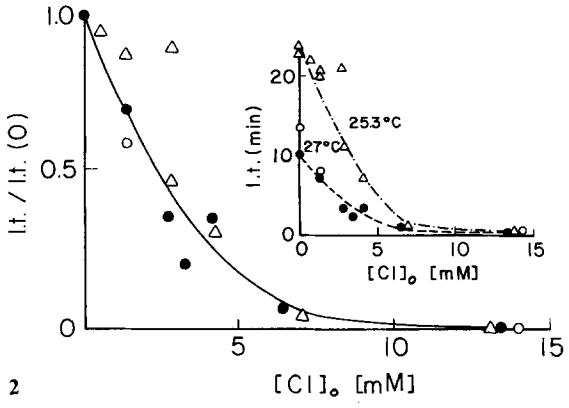

2

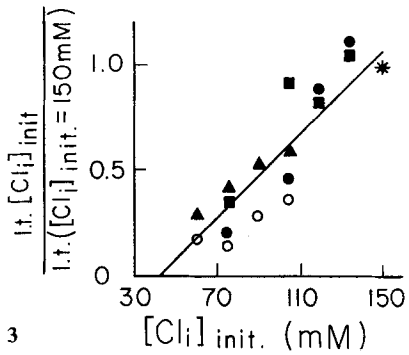

3

Fig. 2. Effect of Cl concentration in the medium (Cl_o) on the latent time (l.t.) of NBD-taurine efflux ($Cl_i - SO_{4_o}$ conditions). Cl-loaded cells pre-equilibrated with 150 mM NaCl, 20 mM phosphate, pH 7.4, and loaded with NBD-taurine (1 mM) were washed twice with ice-cold CO_2-free sulfate medium (110 mM Na_2SO_4, 20 mM phosphate, pH 7.4) and jetted into a fluorimeter cuvette containing the same sulfate medium supplemented with the indicated concentrations of Cl (as NaCl). Fluxes were conducted at the following temperatures: 27 °C (○, ●) and 25.3 °C (△). The relative latent time (l.t./l.t. (0)) was determined as described in Fig. 1 (l.t. represents the latent time at any given Cl_o, and l.t. (0) represents l.t. at $Cl_o = 0$). The calculated l.t. values are shown in the inset. The $[Cl_o]$ which induced a 50% reduction in l.t. (relative to l.t. (0)) were 2.0 and 2.5 mM at 27 and 25.3 °C, respectively

Fig. 3. Effect of Cl_i substitution for SO_{4_i} on the latent time of NBD-taurine efflux ($Cl_i - SO_{4_o}$ conditions). Red blood cells were pre-equilibrated with media composed of mixtures of two isoosmotic solutions: 150 mM NaCl, 10 mM MES, pH 6.9, and 110 mM Na_2SO_4, 10 mM MES, pH 6.9. The pH value of 6.9 was selected in order to set the transmembrane concentrations of anions at a Donnan ratio of 1 at 20 °C [7]. The cells were loaded with 1 mM of NBD-taurine in the same media, and the efflux of the probe was followed by the CMTF method. The latent period was measured at 3 different temperatures as described in Fig. 1: 21.5 °C (■), 28 °C (○, ●) and 32.3 °C (▲). All fluxes were performed with SO_{4_o} media bubbled with N_2 (CO_2-free), except for system (○) which was not CO_2-free. The calculated values of l.t. for the $Cl_i(o) = 150$ mM system were: 45 min (21.5 °C), 9.7 min (28 °C, CO_2-free), 7.3 min (28 °C) and 2.1 min (32.3 °C). Data are given as l.t. relative to the l.t. found at $Cl_i(0) = 150$ mM at the indicated temperature. The linear least-squares fit through the points gave an x-intercept of 43 ± 8 mM ($r^2 = 0.83$, $N = 20$)

marked reduction in the length of the latent phase (Fig. 2). The external concentration of Cl which was required at 25–27 °C, pH 7.4, to reduce l.t. to zero was approximately 12.5 mM and to half the value found at $Cl_o = 0$ (i.e. $l.t._{50}$) was 2.3 ± 0.3 mM. The latter value was similar to the $K^{Cl}_{1/2\text{-out}}$ value of 2.2 ± 0.3 mM found by Gunn and Frohlich [12] as the Cl_o required to stimulate tracer Cl^- efflux to half its maximal value. Although the experimental conditions in our work are not identical to those of the other investigators [12], the observed similarity between their $K_{1/2}$ value for Cl exchange and our $Cl_o(l.t._{50})$ value may indicate a common feature of the transport mechanism. While the above authors attached to $K_{1/2}$ an apparent affinity character for $E - Cl_o$ formation, we are not certain that this necessarily applies to the $Cl_o(l.t._{50})$ observed under the present heteroexchange conditions (Fig. 2).

The complementary experiments, devised to study the effect of internal Cl on the skewness of the transmembrane distribution of E, and consequently on l.t. of NBD-taurine efflux into sulfate medium, are shown in Fig. 3. The experiments were conducted at three different temperatures with cells containing various Cl concentrations substituted isoosmotically by sulfate. The data show the dependence of the latent period on the chloride concentration initially present in cells $[Cl_i(o)]$ and are given in terms of l.t. found at the different $Cl_i(o)$ relative to l.t. found at $Cl_i(o) = 150$ mM. The data display an apparently linear decrease in l.t. with increasing $Cl_i(o)$. The calculated $Cl_i(o)$ at which l.t. was no longer measurable according to the present method of calculation (Fig. 1) was 45 mM at pH 6.9 for the three different temperatures. This concentration provides a minimal estimate for the internal concentration of Cl_i required to induce a latent phase. However, whether or not this is the value attained also at the end of the latent time in $Cl_i - SO_{4_o}$ conditions (i.e., $Cl_i(o) = 150$ mM, $SO_{4_o} = 100$ mM) remains to be demonstrated by direct measurements of Cl_i with time. Nevertheless, our interpretation is that the l.t. represents a phase in which the skewed distribution of carrier is maximal and constant

with time, so that SO_4 flux into cells ($J_{in}^{SO_4}$) in exchange for Cl_i is expected to be independent of Cl_i. We can represent that mathematically by the following empirical relationship:

$$\text{l.t.} = \frac{[Cl_i(o) - Cl_i\text{-crit}]}{J_{in}^{SO_4}} \frac{V_{cell}}{A_{cell}} \quad (5)$$

where $Cl_i(o)$ is the initial Cl concentration in cells (in mM), Cl_i-crit is Cl_i at the end of the latent time, V/A the cell-volume to cell-surface ratio and $J_{in}^{SO_4}$ the inward flux of sulfate during the latent time. This interpretation provides a reasonable explanation for the apparently linear relationship between l.t. and $Cl_i(o)$ (Fig. 3). However, at present, the above relationship should be regarded as semiquantitative, since the l.t. values used for its construction are only estimates of the true l.t.'s. The latter arises from the difficulty in selecting the best graphical method for the determination of l.t. from flux profiles such as those shown in Fig. 1. (*See also* Appendix.)

Since the length of the latent phase is assumed to depend on the rate at which sulfate enters into cells, a reasonable expectation is that the temperature profile of l.t. would be closer to the temperature profile of SO_4 exchange [19] rather than that of Cl exchange. That this is, in fact, the case, is shown in the monophasic nature of the Arrhenius plot of the reciprocal of l.t. plotted versus $1/T$ (T, absolute temperature) (Fig. 4). The calculated E_a for l.t. was 41 ± 2 kcal/mol (170 ± 8 kJ/mol) ($r^2 = 0.98, N = 10$). The E_a calculated for the efflux rate observed after the latent time (a.l.t.) was 36 ± 3 kcal/mol (150 ± 10 kJ/mol) ($r^2 = 0.97$, $N = 8$). These values are closer to those observed for anion self exchange in $SO_{4_i} - SO_{4_o}$ conditions ($E_a = 30 \pm 1$ kcal/mol,) [19] than those observed in $Cl_i - Cl_o$ conditions ($E_a = 23 \pm 3$ kcal/mol) [3]. However, the difference between the E_a value of l.t. and of NBD-taurine transfer in $SO_{4_i} - SO_{4_o}$ conditions is statistically significant. This indicates that in asymmetric conditions there are additional factors that might affect the rate-limiting step of the mechanism, such as the membrane potential and/or the intracellular H^+ concentration created by $H^+ - SO_4$ cotransport into cells [13].

An additional means to modulate the transmembrane distribution of carriers is by varying the pH of cells and medium [15]. Thus, cells loaded with either Cl or SO_4 and NBD-taurine at different pH, were studied with the CMTF method in either isoosmotic Cl or isoosmotic SO_4 media (Fig. 5). The pH profiles are presented in terms of initial rates of NBD-taurine transfer normalized to 1 mM NBD-taurine in order to account for variations of Donnan ratio with pH (*see* Materials and Methods). In $Cl_i - Cl_o$, $SO_{4_i} - SO_{4_o}$ and $SO_{4_i} - Cl_o$ conditions, NBD-taurine fluxes increased with pH up to pH 7.5, and then they either decreased slightly in the 7.5 to 9.0 pH range, as in $Cl_i - Cl_o$, or further increased as in the SO_4 cells. In $Cl_i - SO_{4_o}$ conditions, on the other hand, the pH profiles were considerably more complex, displaying a trend opposed to those observed in SO_4-loaded cells or in Cl-loaded cells in symmetrical conditions.

The normalized initial rate of NBD-taurine efflux

$$\bar{v} = v_{init}/[\text{NBD} - \text{t}]_{init} \quad (6)$$

where v_{init} denotes the initial rate and $[\text{NBD} - \text{t}]_{init}$ the concentration of probe in cells at $t = 0$, was shown in the accompanying work [ref. 9, Eq. (8)] to be proportional to $[E_i]$, the free monovalent form of the carrier in the inward-facing conformation. Thus, the experimental points in Fig. 5 provide a relative measure for the availability of E_i sites at any given condition of pH and anion composition. In $Cl_i - Cl_o$ conditions, $[E_i]$ increased with pH, mainly due to two factors: a decrease in the amount of protonated E [11], and the Donnan effect [7]. The leveling off in alkaline pH can be explained by the same factors which were invoked to determine the pH profile of Cl self-exchange [4, 15].

The pH behavior in SO_4-loaded cells is considerably different from that of Cl-loaded cells. In $SO_{4_i} - SO_{4_o}$ conditions the effect of pH on $[E_i]$ due to protonation of E and due to the Donnan effect is much more pronounced than observed in $Cl_i - Cl_o$ conditions. This is in accord with the recent findings of Milanick and Gunn [17] that the affinity of SO_4 for the protonated form of the carrier is an order of magnitude higher than that for the unprotonated form. Thus, in the case of SO_4, the effects of changes in protonation and in Donnan ratio are multiplicative rather than additive as in the case of Cl. The pH profile in $SO_{4_i} - SO_{4_o}$ conditions is, therefore, much steeper than that obtained in $Cl_i - Cl_o$ conditions. In $SO_{4_i} - Cl_o$ conditions, the pH profile is similar to that obtained in symmetric SO_4 conditions, except

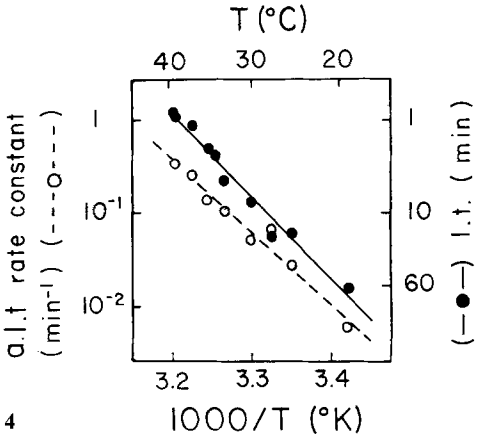

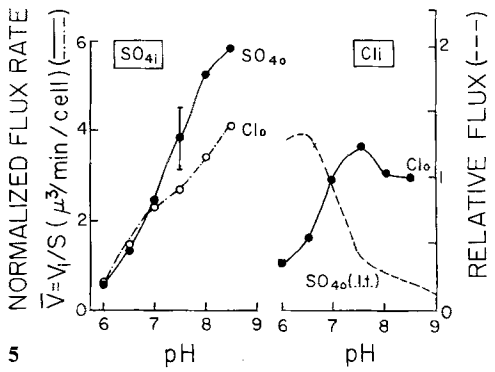

Fig. 4. Temperature dependence of NBD-taurine efflux under asymmetric $Cl_i - SO_{4o}$ conditions. Red blood cells equilibrated in Cl medium (150 mM NaCl, 10 mM HEPES, pH 7.4) were loaded with 1 mM of NBD-taurine. The efflux of the fluorescent probe into SO_4 medium (110 mM Na_2SO_4, 10 mM HEPES, pH 7.4) was monitored fluorimetrically at the indicated temperatures. The latent time l.t. was measured for each temperature as described in Fig. 1. The rate constant of efflux obtained after the latent time (a.l.t.) was determined as $[dF/dt]/[F(\infty)-F(o)]$, where $[dF/dt]$ is the slope of the linear phase of the efflux trace and $[F(\infty)-F(o)]$ is the total change in fluorescence intensity between time zero and infinity. The energy of activation values (E_a) were calculated from the linear least-squares fit of the experimental points: E_a (l.t.) = 41 ± 2 kcal/mol (170 ± 8 kJ/mol) ($r^2 = 0.98$, $N = 10$) and E_a (a.l.t.) = 36 ± 3 kcal/mol (150 ± 10 kJ/mol) ($r^2 = 0.97$, $N = 8$)

Fig. 5. pH dependence of NBD-taurine efflux. Red blood cells were pre-equilibrated in either chloride (150 mM NaCl, 10 mM Tris, 5 mM HEPES, 5 mM MES) or sulfate (110 mM Na_2SO_4 replacing the NaCl above) media at the indicated pH values and were subsequently loaded with NBD-taurine (1 mM external concentration). The cells were washed twice with ice-cold isotonic Na_2SO_4 to remove extracellular probe, and were injected into a fluorimeter cuvette containing either the chloride (Cl_o) or sulfate (SO_{4o}) media at the indicated pH. NBD-taurine efflux was followed by the CMTF method and the initial flux was corrected for variations in internal probe concentration at Donnan equilibrium (cf. Materials and Methods). The profile of the normalized initial rates of efflux $\bar{v} = v_i/S_i$ (30 °C) from either Cl-loaded cells (Cl_i) (*right*) or SO_4-loaded cells (SO_{4i}) (*left*) are shown as a function of external pH. The display of the data in terms of $\bar{v}$ is justified, inasmuch as $\bar{v} \propto E_i$ (cf. text) in all the above experimental conditions. For $Cl_i - SO_{4o}$ conditions we calculated the kinetic parameters as the reciprocal of the normalized latent time (l.t.) given as $v_{l.t.} = V_{cell} \times r \times 150/\text{l.t.}$, where V_{cell} and r are the experimentally determined red cell volume and Donnan ratio, respectively. The value of $v_{l.t.}$ is given in units relative to the value observed at pH 7.0

that at alkaline pH values the pH dependence is less pronounced. However, this could be accounted for by the fact that some Cl might have entered the cells and competed with NBD-taurine for E_i sites. The competition with Cl vis-à-vis SO_4 is expected to be more effective at relatively higher pH values.

The pH profile found in $Cl_i - SO_{4o}$ conditions shows a different aspect of the anion exchange mechanism. As discussed above, the l.t. gives a measure for the time required for a discrete amount of Cl_i (e.g., 150–45 mM at 20 °C, pH 6.9) to be exchanged by SO_4. Thus, the reciprocal of l.t., or rate of l.t. (i.e., $V_{cell}[Cl_i]/\text{l.t.}$) is closely related to the rate of SO_4 influx, the rate-limiting step in these experimental conditions. This relationship provides an explanation for the close resemblance found between the pH profile of l.t. (Fig. 5) and that of SO_4 self-exchange [20].

Finally, an interesting feature of NBD-taurine as a probe for the anion exchange system emerges from the similarities found in the pH profiles of NBD-taurine transfer and those of inorganic anion self-exchange. This is reflected not only in $Cl_i - Cl_o$ conditions, but also in asymmetric $Cl_i - SO_{4o}$ conditions. In the first, the pH profile of NBD-taurine efflux closely follows that of Cl self-exchange [6], whereas in the second, the pH profiles of l.t. rate follows that of SO_4 self-exchange [20]. The various kinetic factors involved in determining these profiles were given above.

Inhibition of NBD-Taurine Transfer in Symmetric and Asymmetric Conditions

A most informative test for assessing the effect of carrier distribution on NBD-taurine transfer profiles resides in the application of the disulfonic stilbene analog DNDS to cells suspended in different media. The compound inhibits equilibrium exchange of anions in an apparently competitive fashion [1] by binding re-

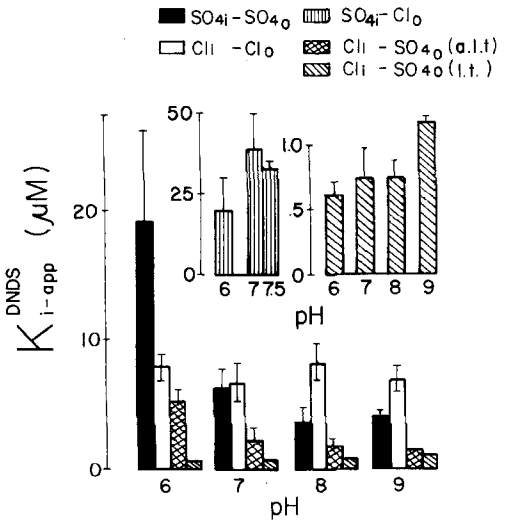

Fig. 6. Susceptibility of the anion exchange system to competitive inhibition by DNDS. Red blood cells were pre-equilibrated in either Cl media (150 mM NaCl, 10 mM Tris, 5 mM HEPES, 5 mM MES) or sulfate media (Na_2SO_4 replacing the NaCl) at the indicated pH values, and subsequently loaded with 1 mM of NBD-taurine dissolved in the same media. NBD-taurine-loaded cells were washed with isoosmotic Na_2SO_4 (5 °C) to remove extracellular probe. They were subsequently injected into a fluorimeter cuvette containing either chloride (Cl_o) or sulfate (SO_{4_o}) media (30 °C) at the same pH as the pre-equilibration medium but containing various concentrations of DNDS. The kinetic parameters of NBD-taurine efflux were measured by the CMTF method. The apparent inhibition constant $K^{DNDS}_{I\text{-app}}$ for each experimental condition (i.e., internal anion, external anion, pH) was obtained by linear regression analysis of NBD-taurine rate constant k, according to the Dixon method [21]: For the $Cl_i - Cl_o$ and $SO_{4_i} - SO_{4_o}$ conditions $1/k$ was plotted versus [DNDS], while for the $SO_{4_i} - Cl_o$ conditions the reciprocal of the initial velocity, $1/v_{init}$ was used. For the $Cl_i - SO_{4_o}$ conditions (a.l.t.) the slope of the linear portion of the efflux trace (cf. Fig. 1) was used for estimating the efflux velocity, while for the $Cl_i - SO_{4_o}$ conditions (l.t.) we analyzed the data in terms of latent time versus DNDS concentration

versibly to a discrete number of sites (E_o and/or HE_o) at the outer surface of the cell membrane [2]. The predictions of the model for the distribution of sites in the various experimental conditions is that the highest concentration of outward-facing forms of carrier should be found in $Cl_i - SO_{4_o}$ conditions and the lowest in $SO_{4_i} - Cl_o$ conditions. This should be manifested in the $k_{I\text{-app}}$ of DNDS on NBD-taurine transfer, which is the concentration required to produce 50% inhibition (IC_{50}). It can easily be shown that the following relation holds true (*see* Appendix):

$$\frac{K_{I\text{-app}}}{K_B} = \frac{E_t}{E_s} \tag{7}$$

for K_B being the carrier-DNDS dissociation constant, and E_t and E_s being the total number of transport sites and the number of DNDS-susceptible sites (presumably E_o and /or HE_o), respectively, at any given experimental condition. Since K_B is constant for a given pH and temperature, then $K_{I\text{-app}}$ of DNDS yields a reliable measure of the transmembrane distribution of transport sites (i.e., carriers).

Transport was measured as a function of pH, DNDS concentration and in 4 different modes: $Cl_i - Cl_o$, $SO_{4_i} - SO_{4_o}$, $Cl_i - SO_{4_o}$ and $SO_{4_i} - Cl_o$ (Fig. 6). The $K_{I\text{-app}}$ of DNDS was calculated from linear regression analysis of modified Dixon plots [21] for each pH value and each mode (e.g., $Cl_i - Cl_o$, etc.). For the $Cl_i - SO_{4_o}$ mode, $2K_{I\text{-app}}$ values were computed: one describing the DNDS concentration required to double the l.t. relative to control, and the other describing the DNDS concentration that reduced by half the rate constant in the a.l.t. period. As seen in Fig. 6, significant differences in $K_{I\text{-app}}$ are apparent in the various modes. For the symmetric $SO_{4_i} - SO_{4_o}$ mode, the $K_{I\text{-app}}$ of approximately 4 μM increases somewhat as the pH is decreased from 9 to 7, and increases sharply to about 20 μM as the pH is further decreased to 6. This change in $K_{I\text{-app}}$ follows competitive protection of sulfate anions for transport sites. In the symmetric $Cl_i - Cl_o$ mode, the $K_{I\text{-app}}$ is virtually invariant with pH in the 6 to 9 pH range, giving an average $K_{I\text{-app}}$ of 7 μM. In asymmetric conditions distinctly different profiles are obtained. In the $Cl_i - SO_{4_o}$ mode, the $K_{I\text{-app}}$ in the a.l.t. period shows a pH profile similar to that obtained for $SO_{4_i} - SO_{4_o}$, although values of $K_{I\text{-app}}$ are about one-third lower than those obtained in the symmetric modes. The lowest $K_{I\text{-app}}$ values (less than 1 μM) were obtained for the l.t. period in the $Cl_i - SO_{4_o}$ mode (Fig. 6 inset, right), while the highest $K_{I\text{-app}}$ values were obtained in the initial phase of the $SO_{4_i} - Cl_o$ mode (Fig. 6 inset, left). In the two latter modes the most extreme asymmetric conditions are imposed on the system, causing most of the transport sites to face either inward ($SO_{4_i} - Cl_o$) or outward ($Cl_i - SO_{4_o}$). The marked difference in susceptibility of the transport system to DNDS, as displayed in the $K_{I\text{-app}}$ values (40 μM for $SO_{4_i} - Cl_o$ as compared with 0.5 μM for $Cl_i - SO_{4_o}$ l.t.) is certainly in line with the aforementioned notion of asymmetric transmembrane distribution of transport sites induced by the two major transportable anions. However, from these studies, it cannot be specified which of the two carrier forms E_o and/or the protonated HE_o are involved in DNDS binding and inhibition.

While the analysis of results of NBD-taurine transfer found in this work was based on the interaction of the fluorescent substrate with E_i forms and on the modulation of E_i by anion composition and pH, the explanations given are certainly not unique. For example, under asymmetric $Cl_i - SO_{4_o}$ conditions, a diffusion potential of Cl^- causes the membrane potential to assume at the outer surface a relatively high negative value in $Cl_i - SO_{4_o}$ conditions and *vice-versa* at $SO_{4_i} - Cl_o$ conditions. This could, in turn, either retard or accelerate the transfer of the anionic NBD-taurine, if the latter exits either by a nonmediated diffusion pathway or by a mediated pathway involving translocation of a charged species (i.e., $E-NBD-t^-$, $HE-NBD-t^+$ or E^+). We have therefore attempted to assess this alternative scheme by clamping the membrane potential with the aid of ionophores or lipophilic ions. Gunn and Frohlich [12] had found that in analogous conditions addition of valinomycin had no effect on halide fluxes. In our systems, however, valinomycin accelerated NBD-taurine efflux, irrespective of the $[K^+]_i/[K^+]_o$ ratio, suggesting that the fluorescent substrate crossed the membrane either complexed to valinomycin or by free diffusion through a valinomycin perturbed bilayer (*not shown*). The accelerated portion of the transfer was insensitive to inhibitors of anion exchange such as DNDS or phloretin. Moreover, addition to the outer medium of fast diffusible ions such as CNS^-, TPP^+, TPB^- or NH_4^+ did not cause any appreciable modification of the l.t. in $Cl_i - SO_{4_o}$ conditions (*not shown*). These results corroborate Jennings' previous claims [14] that the membrane potential plays only a minor role in the exchange of anions measured in asymmetric conditions.

Binding of DNDS to Human Red Blood Cells in Symmetric and Asymmetric Conditions

In the previous section we presented evidence which supports the idea that the composition of anions in cells and media determines the transmembrane distribution of transport sites. This was manifested in marked changes in the susceptibility of the transport system to the impermeant DNDS. In the present section we examined whether modulation of the distribution of carriers is also manifested in the availability of the transport sites as measured by DNDS binding to cells in symmetric and asymmetric conditions. In order to minimize transcellular movement of anions we conducted the experiments at 0 °C (pH 7.4). Typical binding data, as shown in Fig. 7, served as a basis for constructing the more classical binding plot depicted in Fig. 7, inset, as well as for computing by nonlinear regression analysis the binding parameters N (number of binding sites/cell) and $K_{B\text{-app}}$, the apparent binding constant (Table). The results obtained with Cl-loaded cells show a close similarity in the values of $K_{I\text{-app}}$ and those of the apparent inhibition constant $K_{I\text{-app}}$ for the corresponding external conditions. This, despite the fact that binding studies were conducted at 0 °C, whereas inhibition studies were conducted at 30 °C.

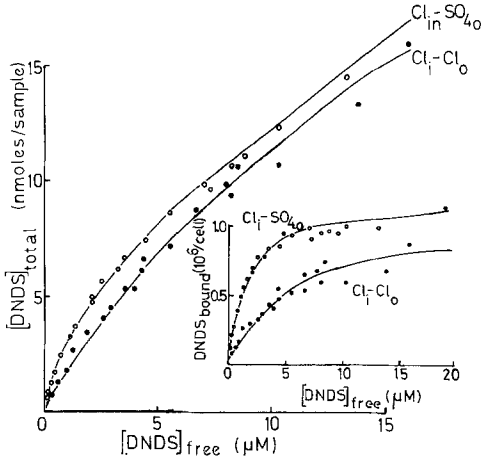

Fig. 7. Binding of DNDS to red blood cells. Red cells washed with and equilibrated in Cl medium (NaCl 150 mM, HEPES 10 mM, pH 7.4), were kept on ice and suspended at this temperature either in the above medium (at 40% hematocrit) ($Cl_i - Cl_o$) or in SO_4 medium (Na_2SO_4 110 mM, HEPES 10 mM, pH 7.4) ($Cl_i - SO_{4_o}$); both media contained various concentrations of DNDS. After a 50-min incubation period in ice-cold conditions, the DNDS remaining in the supernate and the number of cells were determined as in Materials and Methods. The raw binding data are shown in terms of the total amount of DNDS added to the samples ($DNDS_t$) versus the experimentally determined concentration of DNDS in the supernate ($[DNDS]_{free}$). The continuous lines are the computer-derived least-squares fit of the data ascending to: $DNDS_t = [DNDS]_{free} \times \{V + nN/(K_{B\text{-app}} + [DNDS]_{free})\}$ [*see* Eq. (4) in Materials and Methods]. The inset shows the classical saturable component of binding obtained after subtraction of the linear component of the above curves. DNDS bound is given in units relative to the maximal number of specific binding sites. The computed binding parameters are given in the Table.

For the symmetric $Cl_i - Cl_o$ conditions, transport of Cl is fast both at 0 and at 30 °C [6], so that the apparent affinity constants $K_{B\text{-app}}$ and $K_{I\text{-app}}$ describe a property of the system in steady-state conditions. Since SO_4 entry is the rate-limiting step of transport in asymmetric $Cl_i - SO_{4_o}$ conditions, $K_{B\text{-app}}$ at 0 °C describes a property similar to that of $K_{I\text{-app}}$ found in the

Table. Binding parameters of DNDS to human red blood cells (0 °C, pH 7.4) in symmetric and asymmetric conditions

Internal anion	External anion	$K_{I\text{-app}}$[a] (μM)	$K_{B\text{-app}}$ (μM)	Apparent number of sites $N(10^6/\text{cell})$	$r^2(n)$
Cl	Cl	6.5 ±1.8	5.0 ±0.5	1.04±0.24	0.95 (23)
Cl	SO_4	0.76±0.22	1.45±0.15	0.70±0.30	0.996 (30)
SO_4	SO_4	6.2 ±1.4	1.25±0.95	0.39±0.08	0.996 (30)
SO_4	Cl	22 ±4	NM[b]	<0.1	0.996 (43)

[a] $K_{I\text{-app}}$ from Fig. 6, values obtained at 30 °C, pH 7.0.
[b] NM = not measurable.

The parameters describing DNDS binding to human red blood cells (0 °C, pH 7.4) were obtained from nonlinear least-squares analyses of data shown in Fig. 6, using Eq. (4). The correlation coefficient r^2 and the number of data points n are given in the last column. The experimental data of DNDS binding to SO_4-loaded cells are not shown.

latent phase of NBD-taurine transfer at 30 °C (Fig. 6), except for a possible temperature dependence of K_B. The large reduction in value of both constants as a result of changing Cl_o for SO_{4_o} is clearly in accord with the idea of a skewed distribution of transport sites induced by the presence of an external anion which is slowly transported at 30 °C or virtually not transported at 0 °C.

The similarity of $K_{I\text{-app}}$ and $K_{B\text{-app}}$ values emerges from the identity in the values of E_t and E_{susc} (*see* Eq. 7). This is reflected in the number of DNDS binding sites which were determined for Cl-loaded cells in both Cl_o and SO_{4_o} media (Table), indicating that in those conditions all transport sites become available to DNDS at the outer membrane surface.

With SO_4-loaded cells no transcellular movement of SO_4 anions is expected to occur during the time allowed for binding (ca. 10 min) at 0 °C, so that in these conditions, DNDS binding measures a fixed state of carrier distribution. In the symmetric $SO_{4_i}-SO_{4_o}$ condition at 0 °C only the outward-facing transport site can bind DNDS, while the rest of the sites remain occluded to the probe. This is directly reflected in the reduced number of binding sites and, indirectly, in the value of $K_{B\text{-app}}$. In contrast, at higher temperatures (e.g., 30 °C), SO_4 is translocated so that DNDS binding or inhibition is performed under conditions of dynamic steady state. This is immediately reflected in the availability of all transport sites to DNDS at the outer membrane surface, as reported previously [2] ($N = 0.86 \pm 0.07 \times 10^6$ binding sites per cell at 25 °C). In the asymmetric $SO_{4_i}-Cl_o$ conditions at 0 °C, most of the transport sites are expected to be recruited into the inner surface, thus depleting the outer surface from potential DNDS binding sites. This is clearly demonstrated in the Table which shows no detectable DNDS binding of a specific nature.

Taken *in toto*, the binding studies performed with DNDS corroborate the results of DNDS inhibition of NBD-taurine transfer performed in symmetric and asymmetric conditions. These studies provide direct support to the notion that anion transport sites adopt either inward- or outward-facing conformations, according to the anion composition of the medium [16].

Finally, three pieces of experimental evidence obtained in the present work were found to be compatible with the notion of modulation of the transmembrane distribution of transport sites by the concentrations of anions and of protons in cells and in medium:

1. The phenomenon of latency in NBD-taurine efflux during the exchange of intracellular Cl for external, slowly translocating anions. The latency represents a phase in which most anion transport sites are "recruited" [14] towards the external surface of the membrane.

2. The modulation by anion gradients and by pH of the susceptibility ($K_{i\text{-app}}$) and the apparent affinity ($K_{B\text{-app}}$) of the system to inhibition and binding of DNDS, an impermeant competitive inhibitor of anion exchange[2]. Similar conclusions have been drawn using Cl gra-

[2] As the present work was being reviewed, a comprehensive study of DNDS interaction with red cells in symmetric and asymmetric conditions appeared (O. Frohlich, *J. Membrane Biol.* **65**:111-124, 1982). The study was interpreted in terms of the ping pong model of anion transport. The results of the present work are in good quantitative and qualitative agreement with those of O. Frohlich.

dients and the competitive inhibitor 4,4′-diisothiocyano-2,2′-dihydrostilbene disulfonic acid (H_2DIDS) [16].

3. The modulation of the availability of DNDS binding sites (i.e., anion transport sites) in sulfate-loaded cells at 0 °C.

Since the modulation of the distribution of transport sites is intimately related to the ping-pong mechanism of anion exchange [15, 16], the evidence shown above would seem to support that model [12]. However, the latter does not exclude the possibility that the present work is explainable also in terms of alternative mechanisms, particularly those based on the model of "simultaneous exchange" [14, 15]. Therefore, we proceeded to evaluate the results also on the basis of the latter model. According to this model, the efflux of NBD-taurine is proportional to the concentration of the carrier complex NBD-taurine$_i$-E-A_0, and the translocation rate k_{NA} of this complex

$$k_{\text{inst}}(t) = \frac{V_N}{[N_i]} = \frac{k_{NA} \cdot E_t \cdot [A_o]/(K_{A_o} + [A_o])/K_{Ni}}{1 + [B_i]/K_{Bi} + [A_i]/K_{Ai} + [N_i]/K_{Ni}} \quad (8)$$

where $k_{\text{inst}}(t)$ is the instantaneous rate constant, V_N is the efflux rate, $[N_i]$ is the concentration of internal NBD-taurine at a given time t, E_t is the total concentration of carriers, $[A_o]$ is the concentration of the external anion A which is constant with time, $[N_i]$, $[B_i]$ and $[A_i]$ are the concentrations of internal anions which change with time, and K_{Ai}, K_{Bi} and K_{Ni} are the respective Michaelis constants for the three anions at the inner surface. In the experimental conditions used in this work, $[N_i] \ll K_{Ni}$, so that $[N_i]/K_{Ni}$ is negligible in Eq. (8).

1) Since, during fluxes performed in asymmetric conditions, the numerator in Eq. (8) remains constant with time, it is clear that only marked changes in the denominator could explain the phenomenon of latency according to the simultaneous model. However, denoting sulfate as A and chloride as B in Eq. (8), it was found that changes in $[B_i]/K_{Bi} + [A_i]/K_{Ai}$ with time were at the most by a factor of two. This renders the above explanation untenable.

2) Addition of Cl ions to the external medium in Cl_i:SO_{4_o} conditions, that is introduction of a B_o term in the numerator of Eq. (8), leaves the latter essentially constant with time. This is expected to lead, on one hand, to higher $k_{\text{inst}}(t)$ values, and on the other hand, to an increase in l.t., since the presence of external Cl will competitively inhibit sulfate entry. However, the results shown in Fig. 2 show an opposite behavior to that predicted by the simultaneous model. That is, after addition of Cl_o, NBD-taurine fluxes remain low in the latent phase and the length of l.t. decreases rather than increases.

3) According to the simultaneous model, the number of inward-facing transport sites is expected to be equal to that of outward-facing sites, irrespective of the anion composition of cells and of medium. Therefore, the apparent binding constant and the apparent inhibition constant of probes such as DNDS, which is known to interact only with transport sites facing outward [1, 2], are likely to be affected only by the externally present anions. The data shown in the Table clearly demonstrate that not to be the case. Marked differences are found both in the number of DNDS susceptible sites and in the K-app values for binding as well as for inhibition between symmetric and asymmetric conditions.

Although the three criteria used above provide a firm basis for rejecting the simultaneous model, it is not inconceivable that a more complex simultaneous model could be drawn to fit the data. However, that model would have to incorporate many other features for which hitherto, no experimental evidence is available (e.g., cooperativity between sites, existence of occluded forms of carrier-anion complexes, etc.).

Conclusions

The present work together with the previous one [9], support the following conclusions:

1. In human erythrocytes, NBD-taurine is transported only by the anion transport system.
2. NBD-taurine transport is mediated by the monovalent form of the carrier mechanism.
3. NBD-taurine efflux gives a measure for the concentration of monovalent carriers at the inner membrane surface.
4. NBD-taurine efflux profiles obtained in different pH, temperatures, inorganic anion compositions and in the presence of impermeant inhibitors, are explainable within the framework of the titratable carrier model with asymmetric ping-pong mechanism.
5. Inhibition and binding constants of an impermeant inhibitor give a measure of the car-

riers' concentration (E and/or HE) at the outer membrane surface.

6. The temperature profiles of NBD-taurine efflux under symmetric conditions suggest that a determining step in the carrier function is probably related to binding of the predominant inorganic anion. A possible site of action of the inorganic anion is the anion modifier site.

This work was supported in part by a National Institutes of Health grant GM27753 and by the United States-Israel Binational Science Foundation (BSF), Jerusalem. We are grateful for the excellent technical assistance of Mrs. Y. Keren-Zur, the helpful suggestions of Prof. W.D. Stein and Prof. H. Ginsburg, as well as for the secretarial assistance of Mrs. E. Dicker. O.E. is the recipient of the M. Landau Prize for distinguished PhD. Thesis.

A preliminary account of this work was presented at the Israel Biochemical Society Annual Meeting, 1982, Rehovot, Israel, *Isr. J. Med. Sci.* **18**:*S5*.

Appendix A

Simulation of the Time-Dependent Changes of Internal Cl Concentration, of Internal Carrier Concentration and of NBD-Taurine Egress During Cl_i:SO_{4_o} Exchange[3]

The kinetics of Cl_i:SO_{4o} exchange can be described in terms of the ping-pong mechanism by a set of coupled equations. These equations, which describe the time-dependent changes in Cl_i, SO_{4_i}, NBD-taurine$_i$ and in the various carrier forms E_i, E_o, etc. are solved numerically by a computer program. The detailed derivation of the equations, the description of the computer program and the determination of the kinetic constants are the subject of a forthcoming work (Eidelman et al., *to be submitted*). A basic assumption made is that the rate of carrier egress complexed to internal anions is equal to the rate of carrier ingress complexed to external anions, that is:

$$f^{io}[ECl_i]+g^{io}[HES_i]=f^{oi}[ECl_o]+g^{oi}[HES_o]. \quad (A1)$$

[3] *Glossary of terms used in Appendix A:*

$[Cl_i]$, $[Cl_o]$ – the respective internal and external concentration of Cl.

$[S_i]$, $[S_o]$ – the respective internal and external concentration of SO_4.

$[N_i]$, $[N_o]$ – the respective internal and external concentration of NBD-taurine.

$[H_i]$, $[H_o]$ – the respective internal and external concentration of protons.

$[E_t]$ – the total concentration of anion transport sites.

$[E_i]$, $[ECl_i]$, $[HES_i]$, $[E_o]$, $[ECl_o]$, $[HES_o]$ – the concentration of inward- or outward-facing anion transport sites either in free form or complexed with either Cl or SO_4.

K_{ci}, K_{hsi}, K_{hso} – the respective dissociation constants of the ECl_i, HES_i, HES_o complexes.

K_{Hi}, K_{Ho} – the respective dissociation constants of HE_i and HE_o;

F_i, F_o – the respective amounts of free transport sites facing either inwards or outwards relative to the total amount of transport sites facing the same surface.

V_c – the internal volume of a red cell.

f^{io}, f^{oi}, g^{io}, g^{oi} – the respective molecular rate constants for translocation of the complexes ECl_i, ECl_o, HES_i, HES_o.

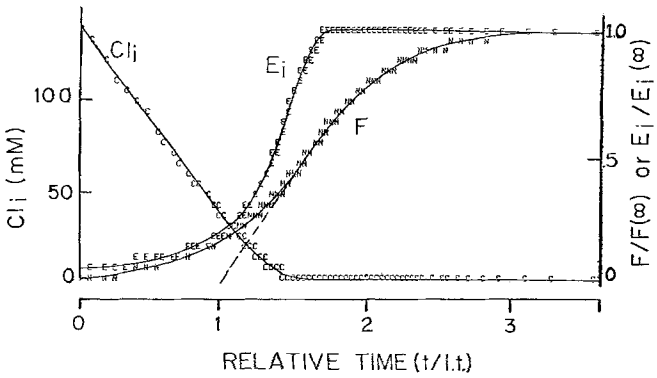

Fig. 8. Computer simulation of the time dependence of E_i, Cl_i and NBD-taurine fluorescence in Cl_i:SO_{4_o} conditions. The relative concentration of E_i, Cl_i and of NBD-taurine fluorescence F are shown as a function of time (t) given on a relative scale (t/l.t., where l.t. is the latent time). The l.t. value extrapolated from the F/F_∞ profile is denoted by the broken lines. The mathematical background for the computer simulation is described in the text

Thus, at any given time, the concentration of free transport sites facing inward (E_i) is determined by the anion composition of the medium and of cells at that time:

$$E_i(t)=\frac{F_i\cdot E_t}{1+\frac{F_i}{F_o}\cdot\frac{f^{io}[Cl_i]/K_{ci}+g^{io}[S_i]/K_{hsi}\cdot[H_i]/K_{Hi}}{g^{oi}[S_o]/K_{hso}\cdot[H_o]/K_{HO}}}. \quad (A2)$$

The efflux rate of Cl is proportional to the concentration of the transportable complex ECl_i, and since the latter is proportional to E_i[9], we obtain

$$\frac{d}{dt}[Cl_i(t)]=-\frac{f^{io}}{V_c}\cdot\frac{[Cl_i]}{K_{ci}}\cdot E_i. \quad (A3)$$

Changes in internal Cl concentration $[Cl_i]$ in short time intervals were computed using Eq. (A3). Computations of changes in $[SO_{4_i}]$ and $[N_i]$ were conducted in an analogous fashion.

A typical simulation of the time dependence of $[Cl_i]$, $[E_i]$ and $[N_o]$ during the process of Cl_i:SO_{4_o} exchange (pH 6.9, 30 °C) is displayed in Fig. 8. The time scale is given in normalized units of time (t) relative to the latent time (l.t.), i.e. (t/l.t.). The initial value of E_i (at $t=0$) was found to be less than 5% of the equilibrium value attained after exit of virtually all Cl_i (at $t\geqq 1.5$ l.t.). Cl was shown to decrease linearly with time for $t\leqq 1.1$ l.t. ($Cl_i\geqq 20$ mM).

The linear decrease of Cl_i was demonstrated experimentally in Fig. 3 and was described empirically by Eq. (5). The pattern of NBD-taurine efflux (F) in these asymmetric conditions is qualitatively similar to the experimental pattern shown in Fig. 1, and underscores the relationship between probe efflux and E_i.

Appendix B

Relationship Between Distribution of Carrier Forms and Apparent Constants of DNDS Binding and of DNDS Inhibition

The interaction of $E+I\rightleftharpoons EI$ leads to a change in the number of carriers populating each of the various forms E_x (E_x

$= E_o$, E_i, HE_i, ECl_i, etc.). The relative distribution of the carrier forms uncomplexed to I remains unaltered so that:

$$\frac{E_x(I)}{E_t - EI} = \frac{E_x(I=0)}{E_t} \tag{B1}$$

where E_t represents the total number of carriers, $[I]$ the concentration of inhibitor and $E_x(I)$ the number of carriers for any particular form (E_i or E_o, etc.) in the presence of a given concentration of I.

From mass law considerations it follows that

$$EI = \frac{[I]}{K_B} E_s(I) \tag{B2}$$

where K_B is the binding constant to the I-susceptible carrier form E_s (E_o and/or HE_o).

Substitution of E_x for E_s in Eq. (B1) and combining Eqs. (B1) and (B2) leads to

$$EI = \frac{[I] \cdot E_t}{\frac{E_t}{E_{s(o)}} \cdot K_B + [I]}. \tag{B3}$$

This is a classical Michaelis expression for probe binding i.e.

$$EI = \frac{E_t[I]}{K_B^{app} + [I]} \qquad K_B^{app} = K_B \frac{E_t}{E_{s(o)}} \tag{B4}$$

or inhibition

$$EI = \frac{E_t[I]}{K_I^{app} + [I]} \qquad K_I^{app} = K_B \frac{E_t}{E_{s(o)}}. \tag{B5}$$

Equation (7) shown in the text is derived immediately from either Eq. (B4) or (B5):

$$\frac{K_{I\text{-app}}}{K_B} = \frac{E_t}{E_s} \quad \text{and} \quad \frac{K_{B\text{-app}}}{K_B} = \frac{E_t}{E_s}. \tag{B6}$$

References

1. Barzilay, M., Cabantchik, Z.I. 1979. Anion transport in red blood cells. II. Kinetics of reversible inhibition by nitroaromatic sulfonic acids. *Membr. Biochem.* **2**:255–281
2. Barzilay, M., Cabantchik, Z.I. 1979. Anion transport in red blood cells. III. Sites and sidedness of inhibition by high affinity reversible binding probes. *Membr. Biochem.* **2**:297–322
3. Brahm, J. 1977. Temperature-dependent changes of chloride transport kinetics in human red cells. *J. Gen. Physiol.* **70**:283–306
4. Cabantchik, Z.I., Knauf, P.A., Rothstein, A. 1978. The anion transport system of the red blood cell: The role of membrane protein evaluated by the use of "probes". *Biochim. Biophys. Acta* **515**:239–302
5. Cleland, W.W. 1963. The kinetics of enzyme-catalyzed reactions with two or more substrates or products. I. Nomenclature and rate equations. *Biochim. Biophys. Acta* **67**:104–137
6. Dalmark, M. 1975. Chloride transport in human red cells. *J. Physiol. (London)* **250**:39–64
7. Dalmark, M. 1975. Chloride and water distribution in human red cells. *J. Physiol. (London)* **250**:65–84
8. Eidelman, O., Cabantchik, Z.I. 1980. A method for measuring anion transfer across red cell membranes by continuous monitoring of fluorescence. *Anal. Biochem.* **106**:335–341
9. Eidelman, O., Cabantchik, Z.I. 1983. The mechanism of anion transport across human red blood cell membranes as revealed with a fluorescent substrate. I. Kinetic properties of NBD-taurine transfer in symmetric conditions. *J. Membrane Biol.* **71**:141–148
10. Eidelman, O., Zangvill, M., Razin, M., Ginsburg, H., Cabantchik, Z.I. 1981. The anion transfer system of erythrocyte membranes: NBD-taurine, a fluorescent substrate analog of the system. *Biochem. J.* (Molecular Aspects) **195**:503–513
11. Gunn, R.B. 1972. A titratable carrier model for both mono- and di-valent anion transport in human red blood cells. *In*: Oxygen Affinity of Hemoglobin and Red Cell Acid-Base Status. M. Rorth and P. Astrup, editors. pp. 823–827, Munksgaard, Copenhagen
12. Gunn, R.B., Frohlich, O. 1979. Asymmetry in the mechanism for anion exchange in human red blood cell membranes: Evidence for reciprocating sites that react with one transported anion at a time. *J. Gen. Physiol.* **74**:351–374
13. Jennings, M.L. 1978. Characteristics of CO_2-independent pH equilibration in human red blood cells. *J. Membrane Biol.* **40**:365–391
14. Jennings, M.L. 1980. Apparent "recruitment" of SO_4 transport sites by the Cl gradient across the human erythrocyte membrane. *In*: Membrane Transport in Erythrocytes. U.V. Lassen, H.H. Ussing, and J.O. Wieth, editors. pp. 450–463, Munksgaard, Copenhagen
15. Knauf, P.A. 1979. Erythrocyte anion exchange and the band 3 protein: Transport kinetics and molecular structure. *Curr. Top. Membr. Transp.* **12**:249–363
16. Knauf, P.A., Tarshis, T., Grinstein, S., Furuya, W. 1980. Spontaneous and induced asymmetry of the human erythrocyte anion exchange system by chemical probes. *In*: Membrane Transport in Erythrocytes. U.V. Lassen, H.H. Ussing, and J.O. Wieth, editors. pp. 389–403, Munksgaard, Copenhagen
17. Milanick, M.A., Gunn, R.B. 1982. Proton-sulfate cotransport: mechanism of H^+ and sulfate addition to the chloride transporter of human red blood cells. *J. Gen. Physiol.* **79**:87–113
18. Passow, H., Kampmann, L., Fasold, H., Jennings, M., Lepke, S. 1980. Mediation of anion transport across the red blood cell membrane by means of conformational changes of the band 3 protein. *In*: Membrane Transport in Erythrocytes. U.V. Lassen, H.H. Ussing, and J.O. Wieth, editors. pp. 345–372. Munksgaard, Copenhagen
19. Schnell, K.F. 1972. On the mechanism of inhibition of the sulfate transfer across the human erythrocyte membrane. *Biochim. Biophys. Acta* **282**:265–276
20. Schnell, K.F., Gerhardt, S., Schöppe-Fredenburg, A. 1977. Kinetic characteristics of the sulfate self-exchange in human red blood cells and red blood cell ghosts. *J. Membrane Biol.* **30**:319–350
21. Segel, I.H. 1975. Enzyme Kinetics: Behavior and Analysis of Rapid Equilibrium and Steady State Enzyme Systems. John Wiley & Sons, New York

Received 28 April 1982; revised 19 August 1982